Available online at www.sciencedirect.com
SCIENCE DIRECT®
Microporous and Mesoporous Materials 84 (2005) 84–96
MICROPOROUS AND MESOPOROUS MATERIALS
www.elsevier.com/locate/micromeso

Synthesis of high silica mordenite nanocrystals using *o*-phenylenediamine template

Mohamed Mokhtar Mohamed [a,*], Tarek Mohamed Salama [b], Ibraheem Othman [b], Ibraheem Abd Ellah [b]

[a] *Faculty of Science, Department of Chemistry, Benha University, Benha, Egypt*
[b] *Faculty of Science, Department of Chemistry, Al-Azhar University, Nasser City, Cairo 650371, Egypt*

Received 28 February 2005; received in revised form 4 May 2005; accepted 9 May 2005
Available online 17 June 2005

Abstract

High silica mordenite samples (Si/Al molar ratios 38 and 60) were synthesized hydrothermally at 433 K with the template route method using *o*-phenylenediamine and characterized with several techniques including XRD, FT-IR, TG/DTA, pyridine-FTIR and N_2 adsorption. The effects of Na_2O/SiO_2 ratio, Si/Al ratio, temperature, crystallization time and various templates on mordenite crystallization as well as crystallite size that was smaller than 50 nm, irrespective of varying the parameters were thoroughly investigated. The effect of alkali cations such as Na^+ and K^+ on mordenite crystallization and on thermal stability of the produced mordenite was also investigated. Pyridine adsorption suggests an increase in Lewis acid sites particularly following hydrothermal treatment at 120 °C where at 160 °C both Lewis and Brönsted acid sites in addition to oxidation products, which are indicative of the existence of dual acid–base sites, were exposed. Surface texturing of the produced samples were correlated with their thermal analyses data.

Keywords: Mordenite; *o*-Phenylenediamine template; Nanocrystals; Characterization; Pyridine-FTIR

1. Introduction

Mordenite is an industrially important zeolite used as a solid catalyst for various reactions such as hydrocarbon hydrocracking, hydroisomerizations, alkylation, reforming and dewaxing [1–4]. There have been lot of works concerning mordenite synthesis in the absence or presence of organic templates as structure directing agents that tailor pore openings for some selected catalytic reactions [5–7]. Nano ($\leqslant$100 nm) sized large (>500 μm) crystal types of mordenite have been synthesized by conditioning the gel composition, crystallization time and templates [8,9]. Mordenites shape selectivity, acidity and thermal stability which are unique features that attract researchers to optimize such parameters for the purpose of achieving highly shape-selective products. Therefore, mordenite dealumination was performed in most cases to increase the Si/Al ratio; increasing the acid sites strength, and creating intracrystalline mesopores [10,11]. However, dealumination sometimes pose problems which most importantly are incomplete amorphization of the structure and presence of defect sites. Additionally, mesoporosity is sometimes disadvantageous for shape selective catalysis. Thus, direct hydrothermal synthesis of catalytically active H-mordenite [12] beyond Si/Al molar ratio of 6.0 in the synthesis gel devoid of other impurity phases is highly desirable. Specialized synthesis conditions in the

* Corresponding author. Present address: Faculty of Applied Science, Umm-Al Qurra University, Kingdom of Saudi Arabia–Makkah Al Mukarramah, P.O. Box 6503 unit 71. Tel./fax: +966 02 5274264.
E-mail address: mohmok2000@yahoo.com (M.M. Mohamed).

1387-1811/$ - see front matter © 2005 Published by Elsevier Inc.
doi:10.1016/j.micromeso.2005.05.017

presence of template and mineralizer [13,14] have been reported recently to achieve Si/Al = 25 in high silica mordenite. Thus, synthesizing mordenite zeolite at high Si/Al ratios by adopting a new template capable of inducing different textural and acidic properties that might exist during dealumination processes is urgently required. The present paper reports the synthesis of mordenite with new templates at high Si/Al ratios in addition to adjusting the gel compositions and crystallization conditions through optimizing the following parameters: Na_2O/SiO_2 ratio, Si/Al ratio, temperature, crystallization time as well as the effect of alkali cations. Physicochemical properties of the produced samples have been characterized using N_2 adsorption, pyridine adsorption, FT-IR, TG/DTA and XRD measurements.

2. Experimental

2.1. Materials

The materials used were: silicic acid powder, sodium hydroxide pellets (AR 98%), potassium hydroxide pellets (AR 98%), aluminum sulfate (Merck, $(Al_2SO_4)_3{\cdot}16H_2O$), *o*-phenylenediamine, *p*-phenylenediamine, *o*-aminophenol and *p*-aminotoluene (Merck), and commercial H_2SO_4.

Silicic acid and aluminum sulfate were used as Si and Al source, respectively. Concentrated sulfuric acid was used for adjusting the gel pH. Different parameters that were studied to increase crystallinity and to decrease the crystal diameter of mordenite were the effect of Na_2O/SiO_2 ratio, different Si/Al ratios, temperature, effect of crystallization time and the effect of using new templates (*o*-phenylenediamine, *p*-phenylenediamine, *o*-aminophenol and *p*-aminotoluene), which were denoted as OPDA, PPDA, OAP and PAT, respectively and the influence of alkali cations.

2.1.1. Effect of Na_2O/SiO_2

The relative amounts (x) of Na_2O were varied by keeping the other component amounts constant as follows:

$$x\mathrm{Na_2O{:}0.162Al_2O_3{:}}y\mathrm{SiO_2{:}0.185Q{:}100H_2O}$$

where Q is OPDA, with $0.45 \geqslant x/y \leqslant 0.5$.

The hydrogel was prepared by mixing the reagents in the following order:

A specific amount of NaOH was added to silicic acid in a calculated amount of H_2O while stirring, followed by heating at 80 °C until a clear solution was reached. The OPDA, on the other hand, was dissolved in a little amount of H_2O (20 ml) with heating at 50 °C for 20 min. The solution of OPDA along with that of sodium silicate solution was mixed whilst stirring for 15 min. The aluminum sulfate, on the other hand, was dissolved in calculated amount of H_2O with adding 0.5 ml concentrated H_2SO_4 with stirring until a clear solution was reached. To the latter solution, the combined solution of sodium silicate and OPDA was added followed by stirring for 30 min. Then, the pH of the mixture was adjusted to 11 by using NaOH (0.1 M) and H_2SO_4 (0.1 M) solutions. Finally, the mixture was hydrothermally treated at 160 °C in an oil bath, using stainless steal autoclaves, for 6 days. The autoclaves were removed at the specified time from the oil bath and quenched immediately with cold water. The solid product was filtered and washed with distilled water until the pH of the filtrate dropped to 8. The products were dried at 110 °C for 10 h then calcined at 550 °C for 6 h in an air oven.

2.1.2. Effect of SiO_2/Al_2O_3 ratios

The relative amounts of SiO_2/Al_2O_3 were varied according to:

$$3.12\mathrm{Na_2O{:}}y\mathrm{Al_2O_3{:}}x\mathrm{SiO_2{:}0.185Q{:}100H_2O}$$

with $10 \geqslant x/y \leqslant 100$.

The rest of the gel composition parameters are constant. ($Na_2O/SiO_2 = 0.5$, $Q/SiO_2 = 0.0299$ and $H_2O/SiO_2 = 16$ for the entire batch.)

2.1.3. Effect of temperature

The batch of the formula adapted was

$$3.12\mathrm{Na_2O{:}0.162Al_2O_3{:}6.185SiO_2{:}0.185Q{:}100H_2O}$$

The crystallization temperature was varied from 120 °C to 180 °C while the crystallization period was fixed at 6 days.

2.1.4. Crystallization time

The crystallization period was varied from 2 to 6 days during the mordenite synthesis. The temperature was fixed at 160 °C while preparing these batch samples.

2.1.5. Effect of template

The used batch was similar to those mentioned previously and composed of:

$$3.12\mathrm{Na_2O{:}0.162Al_2O_3{:}6.185SiO_2{:}0.185Q{:}100H_2O}$$

With Q = OPDA, PPDA, OAP and PAT. The rest of the gel composition parameters are constant at $Na_2O/SiO_2 = 0.5$, $SiO_2/Al_2O_3 = 38$, $Q/SiO_2 = 0.0299$ and $H_2O/SiO_2 = 16$.

2.1.6. Effect of alkali cations

The used batch was similar to the above

$$3.12\mathrm{N{:}0.162Al_2O_3{:}6.185SiO_2{:}0.185Q{:}100H_2O}$$

where N = K_2O or Na_2O or $Na_2O + K_2O$.

$N/SiO_2 = 0.5$, where silicic acid as silica source, aluminum sulfate as aluminum source and OPDA as

template source was adopted. The temperature was 160 °C and time was 6 days.

2.2. Experimental techniques

The X-ray diffractograms of various zeolitic samples were measured by using a Philips diffractometer (type PW 3710). The patterns were run with Ni-filtered copper radiation ($\lambda = 1.5404$ Å at 30 kV and 10 mA) with a scanning speed of $2\theta = 2.5°\ min^{-1}$. The crystal sizes of the prepared materials were determined using the Scherrer equation. The instrumental line broadening was measured using a LaB_6 standard. The crystallinity of the prepared samples was calculated using the ratio of the sum of the areas of the five most intense peaks for the prepared samples (2θ: 16.8°, 19.6°, 22.2°, 28.2° and 32.3°) to that of the same peaks for the standard (Na-Mordenite Mobil chemicals) and multiplying by 100.

In situ FT-IR spectra of the samples were recorded with a JASCO single beam FT-IR 5300-spectrometer with 50 co-added scans at 2 cm^{-1} resolution. The sample was pressed into a self-supporting wafer and mounted in a quartz infrared cell with CaF_2 windows that connecting to a reduced pressure of 10^{-5} Torr closed circulating Pyrex system with a dead volume of 301 cm^3. The vacuum system was equipped with a vacuum gauge and the experiments were conducted when it leveled to 10^{-5} Torr. The infrared cell was equipped with an electric furnace and the sample temperature was adjusted by using the temperature controller connected to a thermocouple made of nickel chrome. The IR sample was prepared by pressing the catalyst powder ground in an agate mortar to a wafer of ca. 30 $mg\,cm^2$ and then degassed at 300 °C for 3 h before exposure to reacting gases. All IR measurements were carried out at room temperature. All the recorded spectra were presented by subtraction of the corresponding background reference.

The IR spectral changes of pyridine adsorption lie in the region from 1700 to 1400 cm^{-1}. Pyridine (16 Torr) was admitted into the cell and equilibrated with the sample for 30 min. Excess pyridine was then pumped out before recording the spectra. In this way, pyridine was pumped out at 25 and 100 °C each time.

Thermogravimetric and differential thermal analyses (TG/DTA) were carried out using Shimadzu-50 thermal analyzer units. The sensitivity of TG and DTA measurements was 0.01 mg and 25 μv, respectively. In each run about 10 mg of uncalcined sample was heated from room temperature to 1000 °C at a heating rate of 10 °C/min in a current of N_2 flowing at a rate of 30 ml/min.

The nitrogen adsorption isotherms were measured at −196 °C using a conventional volumetric apparatus. The specific surface area was obtained using the BET method. The micropore volume and the external surface area were obtained from the *t*-plot method.

3. Results and discussion

3.1. XRD

3.1.1. Effect of concentration of Na_2O on the formation of zeolite

Fig. 1 shows the diffractograms of the mordenite zeolite produced by changing the Na_2O/SiO_2 ratio in the range 0.45–0.50. This figure includes also the diffractograms of a standard mordenite sample purchased from Mobil Company. The degree of crystallinity of produced mordenite phase increases by increasing the Na_2O/SiO_2 ratio in the range 0.45–0.50. The mordenite phase produced at a ratio of 0.5 exhibits an excellent degree of crystallinity (higher than that of the standard sample). The effect of Na_2O/SiO_2 ratio on different structural parameters of the produced mordenite was investigated.

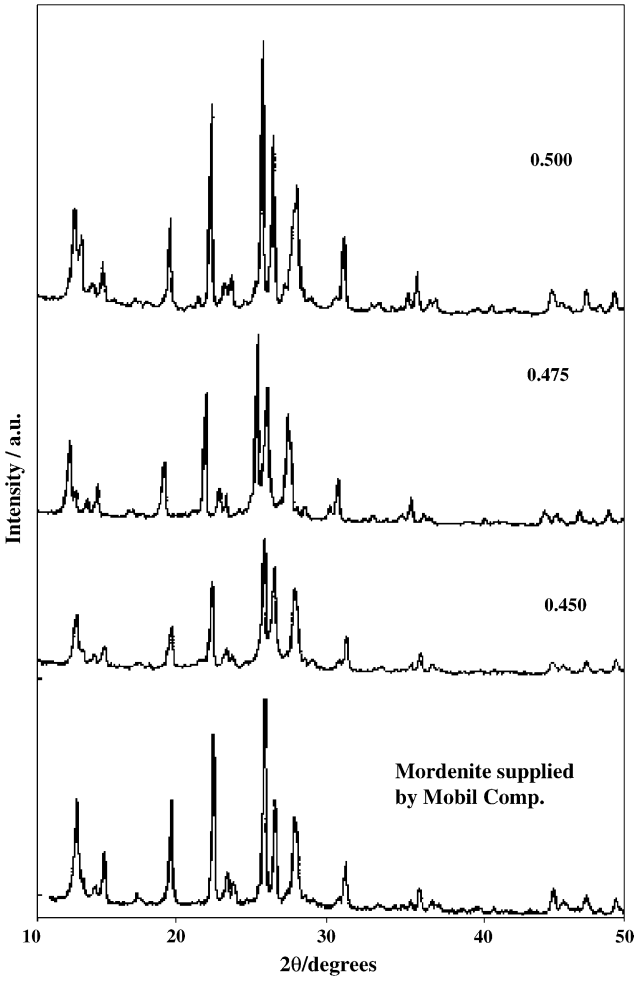

Fig. 1. X-ray diffractograms of synthesized zeolite produced by using different Na_2O/SiO_2 molar ratio.

These parameters that were calculated from the X-ray data are computed together with those of the standard sample and given in Table 1. The various structure parameters of synthesized mordenite samples are near to those of the standard sample. Furthermore, the degree of crystallinity ordering of the mordenite obtained at Na_2O/SiO_2 ratio 0.5 is better than that of the standard sample.

The significant increase in the degree of crystallinity in the produced mordenite due to increasing Na_2O/SiO_2 ratio up to 0.5 could be discussed in terms of the role of OH^- groups in increasing the rate of nucleation of mordenite phase. This increase may lead to an effective decrease in the time necessary for the crystal growth of mordenite phases. Such effect can be explained by a possible increase in the dissolution of the gel phase by increasing the basicity formation of heteronuclei at the expense of the autocatalytic nuclei present in the solid gel. Increasing the crystal size of mordenite as a result of increasing the Na_2O/SiO_2 ratio suggests that Na^+ cation does not play a structure directing role in place of the organic template, delaying the nucleation [15].

3.1.2. Effect of SiO_2/Al_2O_3 ratio on the degree of crystallinity of zeolites

The Na_2O/SiO_2 ratio was fixed at 0.5 and SiO_2/Al_2O_3 was varied between 10 and 100. The diffractograms of the produced mordenite zeolite are depicted in Fig. 2. The decrease in SiO_2/Al_2O_3 ratio from 38 to 10 results in complete collapse of mordenite yielding an amorphous solid. The increase in SiO_2/Al_2O_3 to 25 leads to the formation of a mixture of ZSM-5 and mordenite zeolites, having relatively small degree of crystallinity, which attained a maximum limit at SiO_2/Al_2O_3 of 38 producing only mordenite zeolite. The increase in this ratio up to 60 brought about a significant decrease in the degree of ordering of mordenite without revealing any other competitive phase. At $SiO_2/Al_2O_3 = 100$ the disappearance of the mordenite phase is attained and α-quartz phase is obtained instead.

The different structural characteristics of the solid produced using different SiO_2/Al_2O_3 ratio between 10 and 100 at fixed Na_2O/SiO_2 (0.5) are computed and summarized in Table 2. This table shows that the optimum conditions necessary to obtain mordenite structure

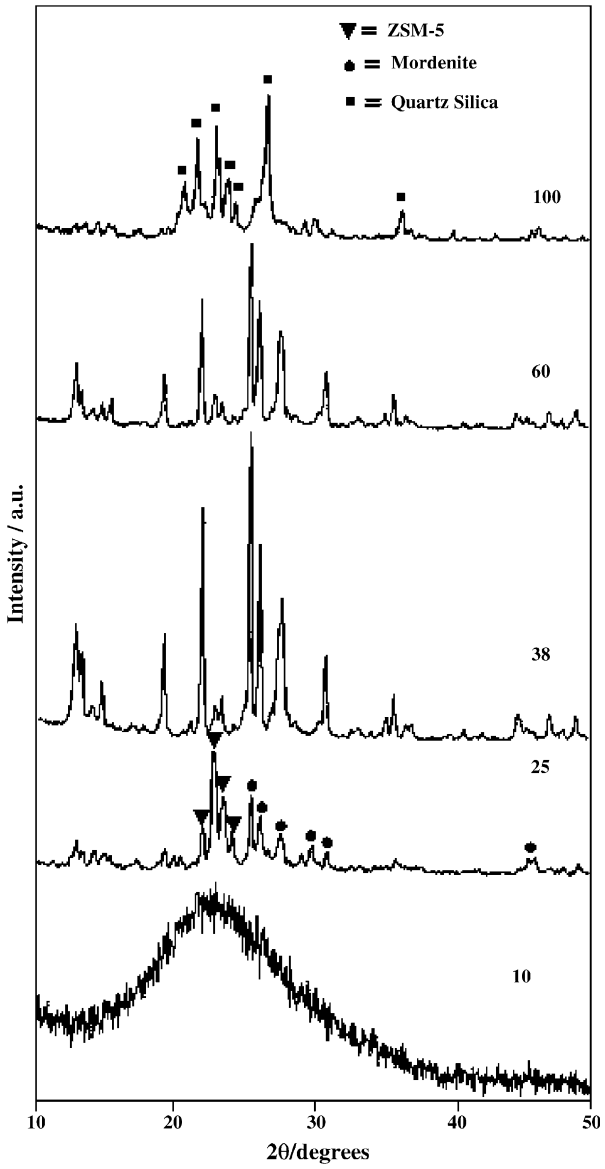

Fig. 2. X-ray diffractograms of synthesized zeolite produced by using different SiO_2/Al_2O_3 molar ratio.

Table 1
The effect of Na_2O/SiO_2 ratio on the particles size and unit cell parameters of the synthesized mordenite zeolite

Na_2O/SiO_2 ratio	D (Å)	Cell parameters (Å)			V (Å)^3	Crystallinity (%)
		a	b	c		
Mordenite (standard)	483.5	18.013	20.678	7.435	27,693.368	58
0.45	342.4	17.940	20.257	7.498	2738.304	45
0.475	444.8	18.325	20.382	7.471	2790.416	64
0.5	484.0	18.129	20.413	7.387	2733.585	100

Note: a, b, c are the lattice parameters (Å), V is the lattice volume (Å)^3; $a*b*c$. D is the particles diameter (Å). The crystallinity percentages were obtained from the sum of the intensities of the 402, 150, 350, 330 and 511 diffraction lines. The standard mordenite sample purchased from Mobil was taken as a reference at 100% crystallinity.

Table 2
The effect of Al_2O_3/SiO_2 ratio on the particle size and unit cell parameters of the synthesized mordenite zeolite

SiO_2/Al_2O_3	Type of zeolite	D (Å)	Cell parameters (Å)			V (Å)^3	Crystallinity (%)
			a	b	c		
10	Amorphous	–	–	–	–	–	–
25	ZSM-5	463.3	19.034	18.047	14.322	4919.727	33
	Mordenite	521.7	16.797	21.058	6.827	2414.787	22
38	Mordenite	484.0	18.129	20.413	7.387	2733.687	100
60	Mordenite	370.1	17.933	20.635	7.515	2780.907	61
100	Quartz silica	–	–	–	–	–	–

having an excellent degree of crystallinity. By fixing Na_2O/SiO_2 at 0.5 and SiO_2/Al_2O_3 at 38. The increase of SiO_2/Al_2O_3 ratio to 60 leads to an effective decrease in both crystal size and degree of crystallinity of mordenite phase that turned entirely to well crystallized silica (α-quartz) at SiO_2/Al_2O_3 of 100.

3.1.3. Effect of hydrothermal temperature on zeolite synthesis

The effect of hydrothermal temperature (in the 120–180 °C range) on the rest of the gel composition parameters that are constant ($SiO_2/Al_2O_3 = 38$, $H_2O/SiO_2 = 16$, $OPDA/SiO_2 = 0.0299$ and $Na_2O/SiO_2 = 0.5$) are thoroughly investigated and presented in Table 3. As the synthesis temperature deviates from 160 °C, the crystal size decreases except that treated at 180 °C. Thus, the temperature of 160 °C is considered as the optimal temperature to obtain mordenite structure having an excellent degree of crystallinity. The raise in temperature during zeolite synthesis up to 180 °C produced a decrease in degree of crystallinity and an increase in crystallite size of the produced mordenite.

3.1.4. Effect of crystallization time on zeolite synthesis

Table 4 illustrates effect of time on the rest of the gel composition parameters, which are constant ($SiO_2/Al_2O_3 = 38$, $H_2O/SiO_2 = 16$, $OPDA/SiO_2 = 0.0299$ and $Na_2O/SiO_2 = 0.5$ and temperature at 160 °C). The time required for crystallization extends to 6 days. The state of art of the nucleation occurs from dissolved precursor species and crystal growth should be thoroughly investigated in more details.

3.1.5. Effect of template on zeolite synthesis

Fig. 3 shows the X-ray diffractograms of the calcination products produced by heating the different zeolitic substrates with a fixed amount of four different kinds of templates. These templates are *o*-phenylenediamine, *p*-phenylenediamine, *o*-aminophenol and *p*-aminotoluene. The hydrothermal conditions of the synthesis process were selected to be at the optimal conditions, i.e. $Na_2O/SiO_2 = 0.5$, $SiO_2/Al_2O_3 = 38$, time = 6 days and temperature = 160 °C. These conditions, as mentioned previously, led to the formation of well-crystallized mordenite. The *o*-phenylenediamine is much better than

Table 3
The effect of hydrothermal treatment on the particle size and unit cell parameters of the synthesized mordenite zeolite

Temperature (°C)	D (Å)	Cell parameters (Å)			V (Å)^3	Crystallinity (%)
		a	b	c		
120	304.7	15.244	20.980	7.383	2361.226	22.73
140	327.2	16.984	19.969	7.415	2514.570	38.20
160	484.0	18.129	20.413	7.387	2733.585	100
180	511.9	18.597	20.039	7.648	2850.087	72.42

Table 4
The effect of time on the particle size and unit cell parameters of the synthesized mordenite zeolites

Time (days)	D (Å)	Cell parameters (Å)			V (Å)^3	Crystallinity (%)
		a	b	c		
2	358.5	17.770	20.865	7.602	2818.602	38
3	472.8	18.182	20.682	7.541	2835.719	76
4	414.0	18.262	19.930	7.539	2743.907	65
5	413.3	18.022	20.592	7.536	2796.678	62
6	484.0	18.129	20.413	7.387	2733.687	100

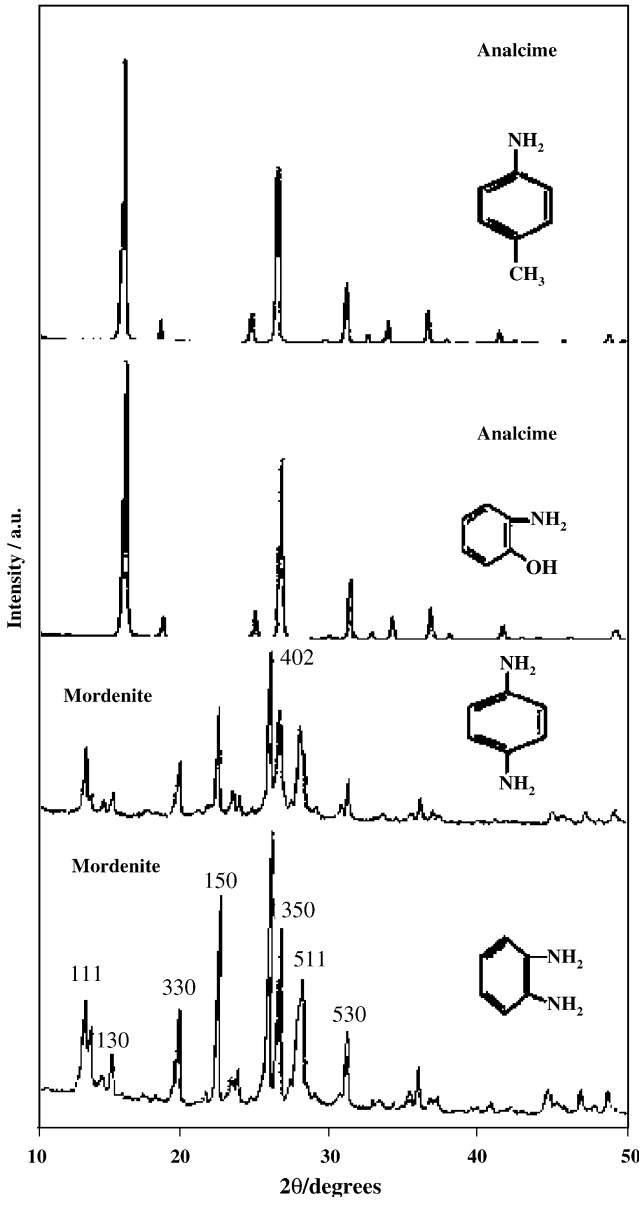

Fig. 3. X-ray diffractograms of different solids precalcined at 550 °C in the presence of different types of templates.

the *p*-phenylenediamine in obtaining well-ordered mordenite structure. The use of the other two templates, *o*-aminophenol and *p*-aminotoluene resulted in the crystallization of another type of zeolitic substrate namely analcime [16]. Analcime is a denser phase with irregular channels formed by highly distorted 8-membered rings and with dimensions 1.6×4.2 Å. The effects of different type of templates on different structural characteristics of the obtained zeolite are summarized in Table 5. The favorable crystallization of analcime using *o*-aminophenol and *p*-aminotoluene could be attributed to their higher basicity comparatively. The superiority of *o*-phenylenediamine over *p*-phenylenediamine in crystallization of mordenite might be attributed to the facile formation of five membered rings in the case of *o*-phenylenediamine template. Although OPDA and PPDA have almost similar sizes but rather varied geometric shapes their filling manners in the channel were different and thus produced different crystallinity.

3.1.6. Effect of Na_2O, K_2O and mixture of both on the mordenite crystallization

Fig. 4 depicts the diffractograms of the mordenite produced using Na_2O, K_2O and equimolar proportion of both after being heated at 550 °C. The optimal conditions for the synthesis process were followed. Fig. 4 shows that Na_2O is much better than K_2O or mixture of $Na_2O + K_2O$ in producing mordenite structure with an excellent degree of crystallinity. This finding can be discussed in terms of some kind of weakening the role of template in the crystallization of mordenite in the presence of K_2O. Such effect may take place via competition between the template and K_2O in bonding with the negative charge of aluminosilicate. The fact that Na_2O is better than K_2O in yielding well crystalline mordenite may suggest that the template can be easily involved in bonding with aluminosilicate in the former due to the smaller size of Na ions in establishing a higher crystallinity comparatively i.e. a fast compensation of negative charges of $(Si–O–Al)^-$ moieties is higher in case of Na. On the other hand, K^+ ions that have larger size diminish the neutralization, which should occur between positive and negative charges, due to the expected competition between K^+ and OPD^+ molecules on negative sites.

On the other hand, these zeolites were subjected to heat treatment at 550, 650, 700, 750 and 800 °C. Upon comparison, the mordenite obtained using Na_2O exhibits an excellent degree of crystallinity upon heating till 550 °C. It undergoes a drastic collapse by heating at 700 °C. In other words, the mordenite prepared using Na_2O showed limited thermal stability. However, the mordenite phase produced using K_2O showed an increase in the degree of crystallinity reaching a maximum limit at 800 °C. Above this temperature, the degree of ordering of mordenite obtained decreases slightly. The revealed thermal stability of mordenite synthesized using K ions than that on using Na ions could be due to the strong interaction of the unpaired electron of K, which is highly unshielded when compared with that of Na. Thus, localizing K ions in zeolite structure as a bulky atom, comparatively, will necessitate higher temperatures to remove it from the structure. In addition, Na^+ is more able to introduce Al into the framework than K^+ does [17] and thus its thermal stability decreases. Furthermore, K ions are known to have strong interaction with oxygen and thus forming superoxide than Na ones that forms only peroxides. This could give a hint to what extent K ions are strongly involved with the oxygen lattice in the framework than Na did.

Table 5
The effect of template on the particle size and unit cell parameters of the synthesized mordenite zeolite

Template	Type of zeolite	D (Å)	Cell parameters (Å)			V (Å)^3	Crystallinity (%)
			a	b	c		
o-Phenylenediamine	Mordenite	484.0	18.130	20.413	7.387	2733.585	100
p-Phenylenediamine	Mordenite	507.5	18.293	24.243	7.359	3263.548	61.0
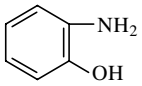 *o*-Aminophenol	Analcime	–	–	–	–	–	–
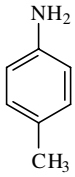 *p*-Aminotoluene	Analcime	–	–	–	–	–	–

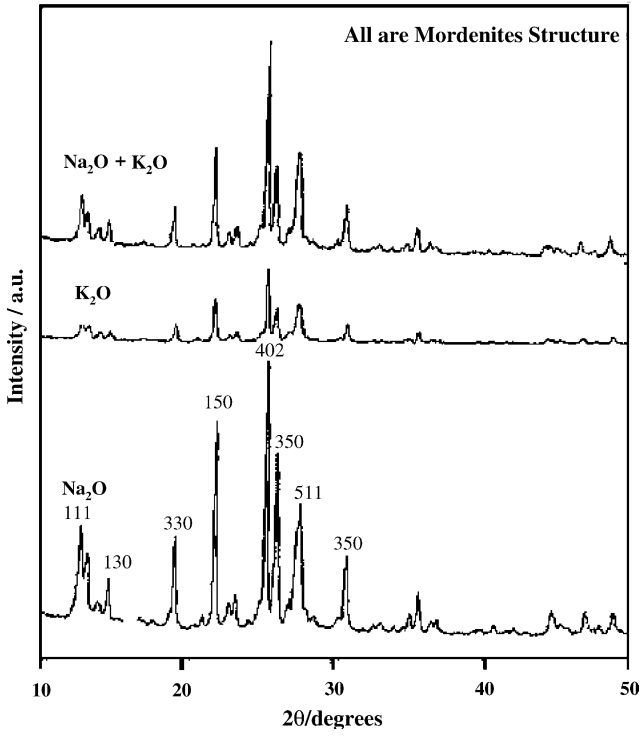

Fig. 4. X-ray diffractograms of Na_2O, K_2O and both of them on (the alkaline/SiO_2 molar ratio kept at 0.5) the produced mordenite.

3.2. Structural properties of synthesized zeolites as traced by FT-IR spectroscopy

The structural characteristics of the synthesized mordenite zeolite produced as a result of increasing the Na_2O/SiO_2 ratio are shown in Fig. 5, in comparison with a reference sample; supplied from Mobil, of similar SiO_2/Al_2O_3 molar ratio (38). The main bands due to asymmetric stretching vibration of νSi–O (at ~1081–1059 cm^{-1}), symmetric stretching vibration of Al–O (at

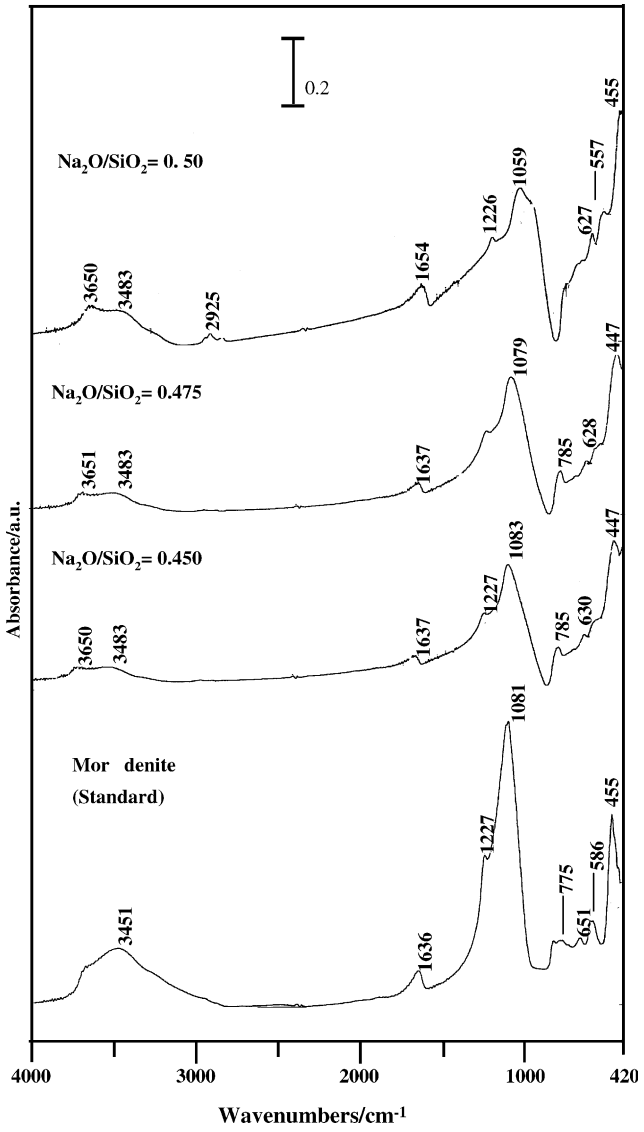

Fig. 5. FT-IR spectra of mordenite synthesized at different Na_2O/SiO_2 molar ratios.

785–775 cm^{-1}), belonging to alternating SiO_4 and AlO_4 tetrahedral and/or single 4-membered rings (at 651–627 cm^{-1}), and vibration of five membered rings (at ~586–557 cm^{-1}) [18,19] are shown as distinct bands at increasing Na_2O/SiO_2 ratio up to 0.5, reflecting a higher crystallinity, comparatively, as exactly concluded from XRD results. A broad band in the hydroxyl region between 3600 and 3300 cm^{-1} with a maximum at ca. 3480 cm^{-1} due to framework SiO–H is seen together with Si(OH)Al groups at 3650 (3648) cm^{-1} characteristic of interaction with the defect sites.

The effect of SiO_2/Al_2O_3 molar ratio on the structural characteristics of the produced mordenite zeolite of fixed Na_2O/SiO_2 ratio (at 0.5) is illustrated in Fig. 6. The bands associated with the structural tetrahedra are clearly seen at SiO_2/Al_2O_3 ratio of 38. However, the lower ratio (25) did not reveal the band at 626 cm^{-1} of Al–O belonging to alternating SiO_4 and AlO_4 tetrahedra where rising up the ratio to 60 brought up a new band at 732 cm^{-1} due to isolated AlO_4 tetrahedra [20]. This points together with the almost vanishing of the 554 cm^{-1} band (T–O in 5-membered rings) to a disturbance in mordenite structure, as has been confirmed previously from XRD results of this sample.

3.3. Thermal analyses

TG and DTA thermograms of the uncalcined mordenite (SiO_2/Al_2O_3 = 38, Na_2O/SiO_2 = 0.5, temperature at 160 °C and time was 6 days) were measured in the temperature range from 25 to 1000 °C and the obtained curves are depicted in Fig. 7. TG indicates a total mass loss of 14.4% that is characterized by several steps of weight loss. DTA, on the other hand, indicates four endothermic peaks at 128 °C, due to desorption of H_2O, and 322 °C, corresponds to elimination of OPDA molecules simply embedded in the aluminosilicate matrix, in addition to peaks at 537 and 877 °C. The peak at 322 °C is different from that corresponding to the decomposition of the organic OPDA (*o*-phenylenediamine $C_6H_4(NH_2)_2$ mp. 103–105 °C). The weight loss indicating OPDA (3.7%) decomposition in the temperature range 300–400 °C is significantly less than that required to form a well defined unit cell (4.75%), assuming four OPDA cations per unit cell in a pure mordenite crystal. This finding could indicate the presence of OPDA molecules enclosed inside micropores of M zeolite. Accordingly, the peak at 537 °C, which is accompanied by a weight loss of 0.88%, may correspond to thermal decomposition of OPDA molecules, which are located in small nanocrystals. However, the high

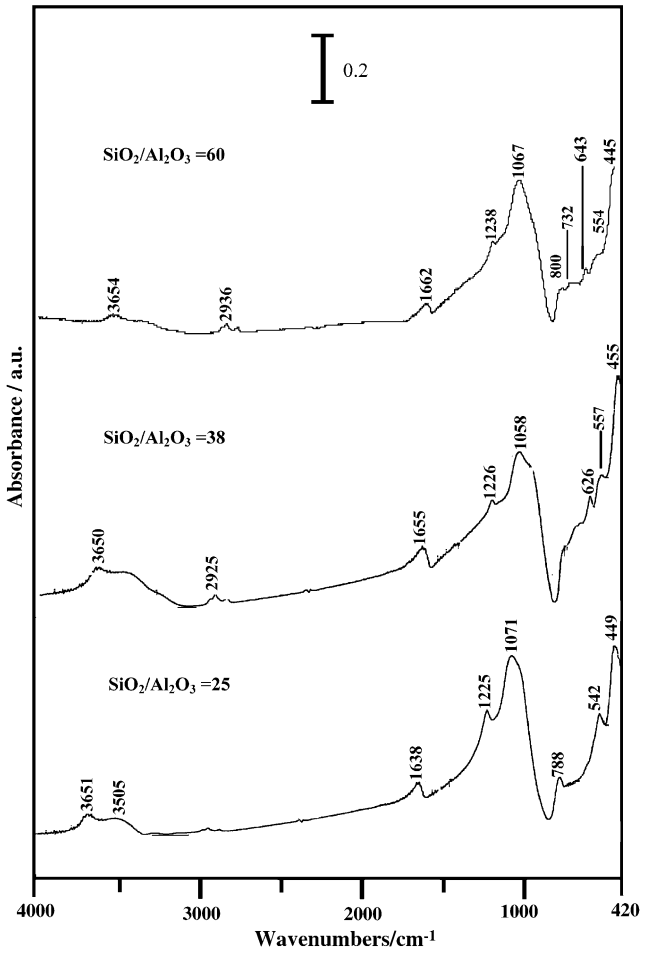

Fig. 6. FT-IR spectra of mordenite synthesized at different SiO_2/Al_2O_3 molar ratios.

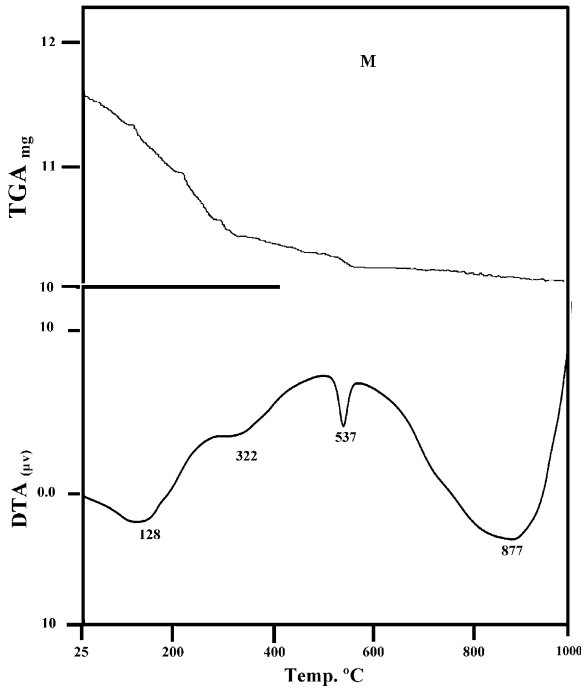

Fig. 7. TGA/DTA curves of mordenite zeolite synthesized at Na_2O/SiO_2 = 0.5 (molar ratio).

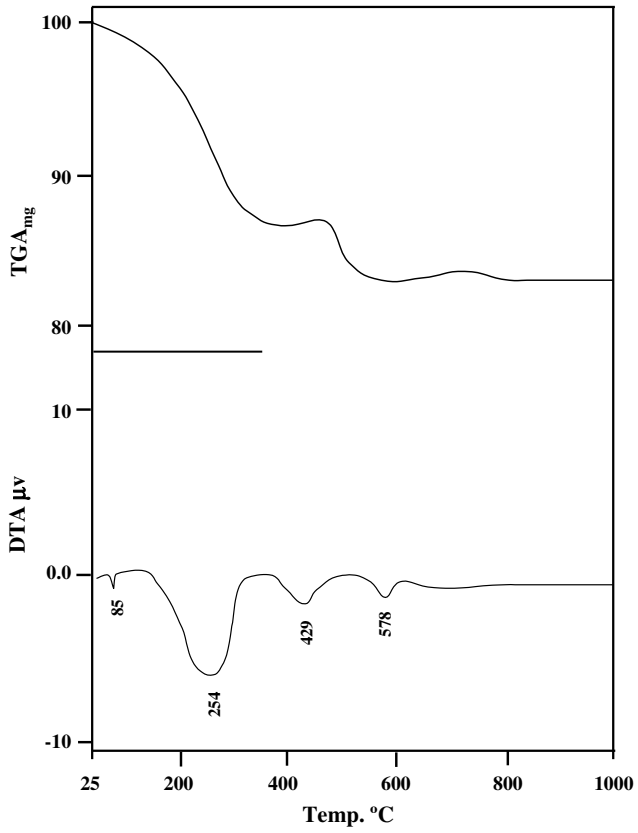

Fig. 8. TGA/DTA curves of mordenite zeolite synthesized by KOH.

temperature peak at 877 °C that corresponds to a weight loss 0.84% could be caused by elimination of H_2O during condensation of surface silanol groups and/or removal of the chemically bound water.

TG and DTA thermograms of the uncalcined mordenite ($SiO_2/Al_2O_3 = 38$, $K_2O/SiO_2 = 0.5$, temperature at 160 °C and time was 6 days) were measured in the temperature range from 25 to 1000 °C and the obtained curves are depicted in Fig. 8. TG indicates a total weight loss of 11.47% that is characterized by several steps of weight loss. DTA, on the other hand, indicates four endothermic peaks at 85, 254, 429 and 578 °C, the peaks at 254 °C, 429 °C and 578 °C correspond to elimination of OPDA molecules simply embedded in the aluminosilicate matrix probably in macropore, mesopore and micropores of mordenite zeolite, respectively.

The comparison between Figs. 7 and 8 show that the shift of the DTA peaks to lower temperature in the sample prepared by KOH (254, 429 °C) were more than those found in the sample prepared by NaOH (322, 537 °C). This indicates that $KOH/SiO_2 = 0.5$ exhibits an appreciable extent of wide pores when compared with $NaOH/SiO_2 = 0.5$. Using K^+ ions instead of Na^+ ones in zeolite synthesis decreases the amount of water used to be desorbed around 100 °C, reflecting the bulky size of K^+ ions. The absence of a peak around 870 °C in the DTA thermograms of the mordenite sample containing Na (Fig. 7) when compared with that containing K indicates the structural stability of the latter comparatively.

3.4. Pyridine adsorption

Fig. 9 shows that Py chemisorbed on mordenite (synthesized at 4 days) zeolite at 120 °C exhibits a simple νCCN spectrum dominated by three strong bands at 1444 (Py), 1490 (LPY + BPy) and 1590 cm^{-1}. The latter band that was assigned to another LPy showed presistance till 280 °C with significant shift into 1600 cm^{-1}. Evacuation of the sample at successive temperatures till 280 °C shows the existence of some newly developed bands at 1530, 1556, 1575, 1596 and 1650 cm^{-1} with simultaneous decrease in LPy band at 1444 cm^{-1}. These former new developments are indeed not due to HPy but

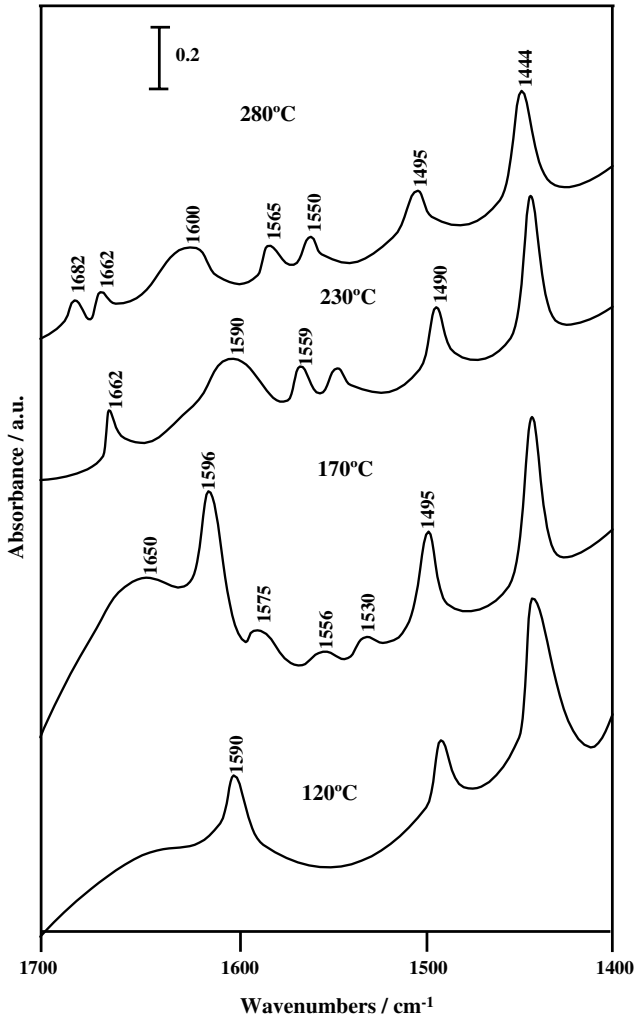

Fig. 9. In situ FT-IR spectra of pyridine adsorption on mordenite (synthesized at $Na_2O/SiO_2 = 0.5$, $SiO_2/Al_2O_3 = 38$, temperature = 160 °C and crystallization time = 4 days). Pyridine was introduced at 120 °C and the spectra were recorded after evacuation for 15 min at different temperatures.

most probably due to Brönsted pyridine (BPy; 1540–1537, 1556, 1650 cm^{-1}) and Py oxidation products (1575 and 1682 cm^{-1}). This indicates the existence of reactive basic OH^-species on Al sites. This implies the existence of dual acid–base pair sites on this sample that was hydrothermally treated for 4 days. Similar results are also reached to the same conclusion upon revealing reactive basic Al–OH groups forming α-pyridone when treated with pyridine [21]. This may suggest the presence of $Al–OH^-$ or $(Si–O–Al)^-$ moieties in appreciable amounts and rather not well compensated by either Na^+ or template or both and thus induced basic properties. The density of acid sites in this sample is four times higher than that devoted from $Na_2O/SiO_2 = 0.45$ at a similar hydrothermal time (not shown).

For the mordenite sample synthesized at high Si/Al ratio (60), Py-FTIR spectra taken at 120, 170 and 230 °C show a large peak at 1444 cm^{-1} ascribed to Py adsorbed on Lewis acid sites (Fig. 10). This band remains unchanged even after desorption at 230 °C together with bands at 1597, 1614 and 1633 cm^{-1} most probably ascribed to same species. A small band at 1650 cm^{-1} indicative of Brönsted acidity was also depicted. The presence of various modes for LPy species assumes different acidity strengths of that site (1597, 1614 and 1633 cm^{-1}).

On mordenite synthesized at 120 °C (Fig. 11) Py uptake gave rise to spectra showing bands 1444, 1491, 1598, 1613 and 1642 cm^{-1} characterizing, respectively, LPy and BPy species. Disappearance of the band at 1613 cm^{-1} and shift of the band at 1642 (1625 cm^{-1}) was observed following outgassing at 275 °C, pointing to the weakness of these sites. Outgassing at 320 °C, retained similar spectrum as that evacuated at 275 °C, reflecting the strength of Lewis acidity of these types and elimination of Brönsted ones.

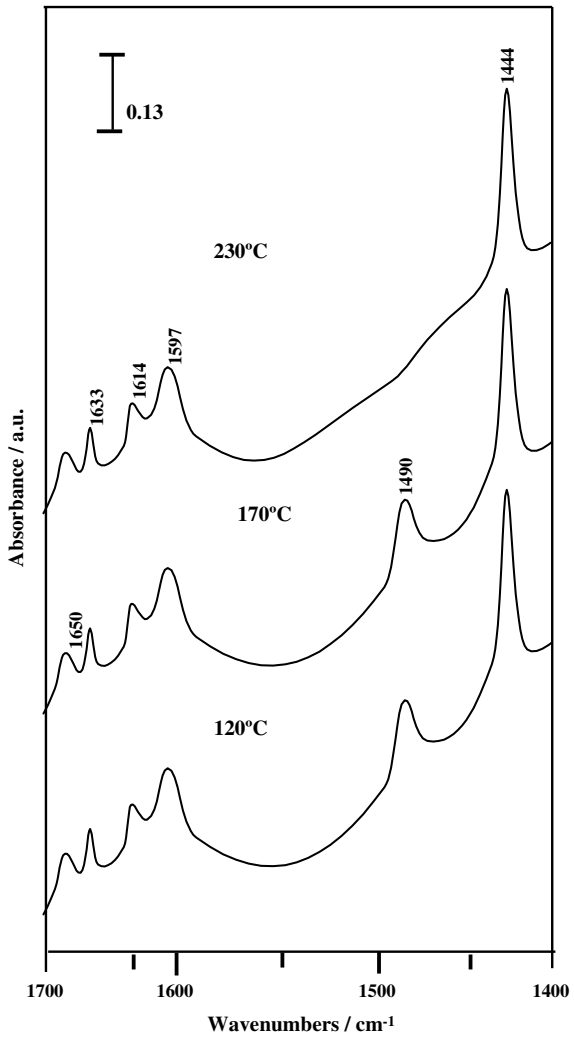

Fig. 10. In situ FT-IR spectra of pyridine adsorption on synthesized mordenite (at $SiO_2/Al_2O_3 = 60$, $Na_2O/SiO_2 = 0.5$, hydrothermal temperature = 160 °C and crystallization time = 6 days). Pyridine was introduced at 120 °C and the spectra were recorded after evacuation for 15 min at different temperatures.

3.5. Surface texture

Surface characteristics of various zeolitic solids were determined from N_2 adsorption isotherm conducted at −196 °C. These characteristics include S_{BET}, S_t, S^{μ}, S^{ext}, S^{wid}, V_p^{total}, and r^-, which respectively correspond to the BET surface area (S_{BET}), statistical surface area (S_t), surface area of micropores (S^{μ}) external surface area (S^{ext}), external surface area of wide pores (S^{wid}), total pore volume of micropores (V_p^{μ}) and mean pore radius (r^-).

The "*t*-plot" method was applied in order to have another estimation of the microporous volume that can be determined by the method developed by Braunauer et al. [22]. The "*t*-plot" method also allows the determination of the external surface of microporous solids; S^{ext}. Based on the observation that, after the complete filling of the micropores only the adsorption on the external surface influences the experimental isotherm, the slope of the straight line of the plot of the volume of the adsorbate against the statistical thickness, is directly proportional to the external surface area of micropores. The intercept for $t = 0$, gives the volume of adsorbate in the micropores (V^{μ}).

Inspection of Table 6 reveals the following: (i) the values of S_{BET} and S_t for various solids investigated are close to each other. This finding indicates the correct choice of the employed *t*-curve and showed the absence of ultramicropores of these solids; (ii) the specific surface areas increase progressively by increase in the Na_2O/SiO_2 ratio, an increase of 16% of the S_{BET} in the Na_2O/SiO_2 ratios from 0.45 to 0.50; (iii) the value of the mean pore radius decreases effectively by increasing Na_2O/SiO_2 ratio from 0.45 to 0.50, a decrease of 33% in the r^- value was observed. This finding may equal the observed increase in the specific surface area of the solid

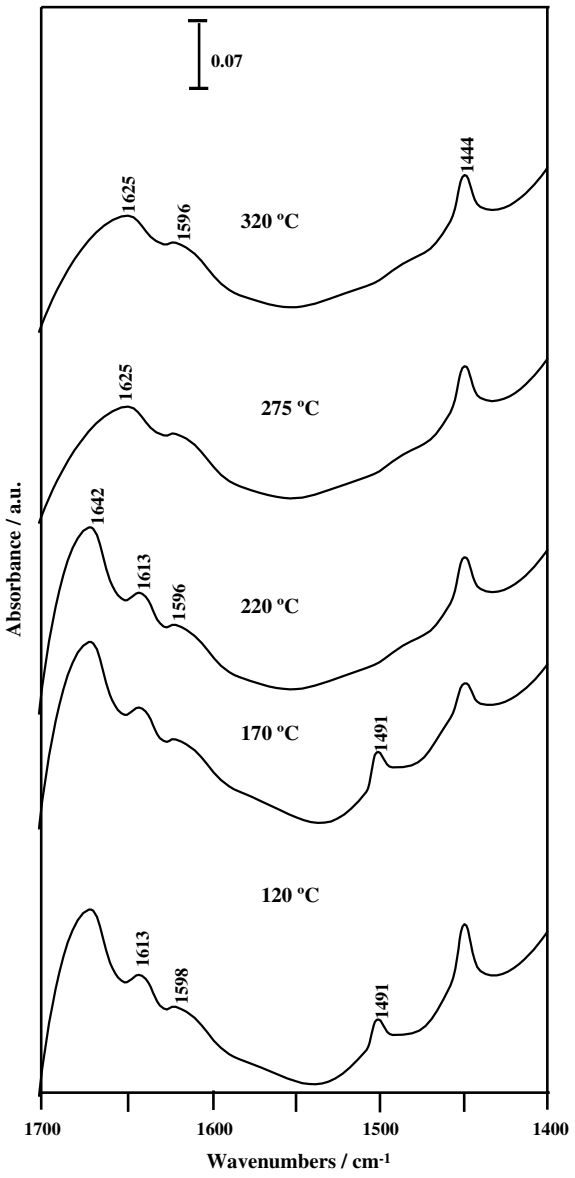

Fig. 11. In situ FT-IR spectra of pyridine adsorption on mordenite (synthesized at hydrothermal temperature = 120 °C, $Na_2O/SiO_2 = 0.5$, $SiO_2/Al_2O_3 = 38$ and crystallization time = 4 days). Pyridine was introduced at 120 °C and the spectra were recorded after evacuation for 15 min at different temperatures.

upon increasing Na_2O/SiO_2 ratio from 0.45 to 0.50; (iv) the external surface area, which includes the surface of particles and the voids decreases to more than one half of S^{ext} initial value at increasing Na_2O/SiO_2 ratio from 0.45 to 0.50; (v) the specific surface area of micropores showed an enhancement by increasing Na_2O/SiO_2 ratio, an increase of 68% in the value of S^{μ} was observed and (vi) the % of contribution of microprosity in S_{BET} increases effectively upon increasing the Na_2O/SiO_2 ratios.

Inspection of Table 7 reveals the following: (i) the values of S_{BET} and S_t for various solids investigated are close to each other for SiO_2/Al_2O_3 at 38, however, for the sample at $SiO_2/Al_2O_3 = 60$, the values of S_{BET} and S_t are varied to each other. This finding indicates the presence of either micropore or ultramicropores in this sample; (ii) the specific surface areas increase progressively by increase in the SiO_2/Al_2O_3 ratios, an increase of 14% of the S_{BET} was found to increase SiO_2/Al_2O_3 ratios from 38 to 60; (iii) the value of the mean pore radius decreases effectively by increasing SiO_2/Al_2O_3 ratios from 38 to 60, a decrease of 25% in the *r*-value was observed according to increasing SiO_2/Al_2O_3 ratios. This finding equals the observed increase in the specific surface area of the solid upon increasing the SiO_2/Al_2O_3 from 38 to 60; (iv) the external surface area which includes the surface of particles and voids decreases markedly by increasing SiO_2/Al_2O_3 ratios from 38 to 60; (v) the specific surface area of micropores is decreased by increasing SiO_2/Al_2O_3 ratios, decrease of 10% in the value of S^{μ} was observed and (vi) the % of contribution of microprosity in S_{BET} decreases specifically by increasing the SiO_2/Al_2O_3 ratios.

Inspection of Table 8 reveals the following: (i) the values of S_{BET} and S_t for various solids investigated are close to each other for temperatures at 120–180 °C. This indicates the correct choice of the employed *t*-curve and rather demonstrates the absence of the ultramicropores in these samples; (ii) the specific surface area increases progressively by the increase in the hydrothermal temperatures, an increase of 20% of the S_{BET} was found by increasing temperature from 120 to 180 °C; (iii) the value of the mean pore radius decreases effectively by increasing the temperature from 120 to 180 °C, a decrease of 18% in the *r*-value was observed with increasing the temperature. This finding equals the observed increase in the specific surface area of the solid upon increasing the hydrothermal temperature from 120 to 180 °C; (iv) the external surface area decreases markedly upon increasing the hydrothermal temperature from 120 to 180 °C; (v) the specific surface area of micropores was found to increase by increasing the hydrothermal

Table 6
Some surface characteristics of different Na_2O/SiO_2 (molar ratio) investigated adsorbents, heated at 300 °C under a reduced pressure of 10^{-5} Torr

Na_2O/SiO_2	S_{BET} (m^2/g)	S_t (m^2/g)	S^{μ} (m^2/g)	S^{ext} (m^2/g)	S^{wid} (m^2/g)	V_p^{total} (cm^3/g)	V_p^{wid} (cm^3/g)	V^{μ} (cm^3/g)	r^-	*C*-const	Microporosity (%)
0.45	279	278	188	84	95	0.467	0.159	0.309	42	13	66
0.475	304	298	205	81	99	0.483	0.155	0.326	40	6	78
0.500	324	323	316	39	8	0.362	0.077	0.285	28	4	89

Table 7
Some surface characteristics of different SiO_2/Al_2O_3 (molar ratio) investigated adsorbents, heated at 300 °C under a reduced pressure of 10^{-5} Torr

SiO_2/Al_2O_3	S_{BET} (m^2/g)	S_t (m^2/g)	S^{μ} (m^2/g)	S^{ext} (m^2/g)	S^{wid} (m^2/g)	V_p^{total} (cm^3/g)	V_p^{wid} (cm^3/g)	V^{μ} (cm^3/g)	r^-	C-const	Microporosity (%)	Type of zeolites
38	324	323	316	39	8	0.362	0.077	0.285	28	4	89	Mordenite
60	369	267	283	24	86	0.303	0.065	0.238	21	3	79	Mordenite

Table 8
Some surface characteristics of different temperature investigated adsorbents, heated at 300 °C under a reduced pressure of 10^{-5} Torr

Temperature (°C)	S_{BET} (m^2/g)	S_t (m^2/g)	S^{μ} (m^2/g)	S^{ext} (m^2/g)	S^{wid} (m^2/g)	V_p^{total} (cm^3/g)	V_p^{wid} (cm^3/g)	V^{μ} (cm^3/g)	r^-	C-const	Microporosity (%)
120	320	309	232	48	88	0.352	0.097	0.255	28	7	72
160	324	323	316	39	8	0.362	0.077	0.285	28	4	79
180	383	318	315	29	68	0.345	0.061	0.284	23	3	82

temperature, an increase comprising of 36% in the value of S^{μ} was observed and (vi) the % of contribution of microprosity in S_{BET} was effectively increased at increasing the hydrothermal temperature.

4. Conclusions

A new templating agent, *o*-phenylenediamine, was well employed in the synthesis of nanometer mordenite crystals (less than 50 nm) with high Si/Al ratios up to 60. Physicochemical properties of the produced mordenite, after optimizing the various synthesis condition to be: $Na_2O/SiO_2 = 0.5$, $SiO_2/Al_2O_3 = 38$, temperature = 160 °C and time of crystallization = 6 days, have shown the following concluding remarks:

(1) The parameters, which most effectively improved mordenite crystallinity as well as decreased the crystal diameter, were principally Na_2O/SiO_2 (0.5) and Si/Al (38) ratios.
(2) Dual acid–base site pairs were developed on mordenites synthesized at 4 days, where on mordenites with Si/Al of 60, the availability of Lewis acid sites was superior to those of Brönsted ones. Thermally stable Lewis acid sites were only attained on mordenites synthesized at hydrothermal temperature of 120 °C.
(3) The involvement of K in mordenites instead of Na was responsible for improving the thermal stability of the produced K-containing mordenite, that showed lower degree of crystallinity than Na-containing mordenite.
(4) Various pore volumes and pore radius were depicted throughout the changed parameters during syntheses of high silica mordenites and as a result various acid sites ranging from dual acid–base, Lewis–Brönsted and Lewis sites were attained. Hence, the mordenite zeolite with tailor made micropores, synthesized with the assistance of *o*-phenylenediamine template showed varied surface texturing as well as acid sites and high crystallinity suggesting an alternative pathway for the synthesis of high silica mordenites that prevailing over those that might exist during dealumination processes.

References

[1] I.V. Mishin, H.K. Beyer, H.G. Karge, Appl. Catal. A 180 (1999) 207.
[2] M.T. Tromp, J.A. Van Bokhoven, M.T. Oostenbrink, J.H. Bitter, K.P. De Jong, D.C. Koningsberger, J. Catal. (2000) 301.
[3] M.M. Mohamed, J. Mol. Catal. A 200 (2003) 301.
[4] S. Samanta, N.K. Mal, P. Kuman, A. Bhaumik, J. Mol. Catal. A 215 (2004) 169.
[5] C. Shao, X. Li, S. Qiu, F. Xiao, O. Terasaki, Micropor. Mesopor. Mater. 39 (2000) 117.
[6] S.D. Kim, S.H. Noh, K.H. Seorg, W.J. Kim, Micropor. Mesopor. Mater. 72 (2004) 185.
[7] M.M. Mohamed, T.M. Salama, I. Othman, G.A. El-Shobaky, Appl. Catal. A 279 (2005) 23;
I. Othman A, PhD Theses, Faculty of Science, Chemistry Department, Al-Azhar University, Nasser City, Cairo, Egypt, 2004.
[8] B.O. Hincapie, L.J. Garces, Q. Zhang, A. Sacco, S.L. Suib, Micropor. Mesopor. Mater. 67 (2004) 19.
[9] Y. Sun, T. Song, S. Qiu, W. pang, J. Shen, D. Jiang, Y. Yue, Zeolites 15 (1995) 745.
[10] M.M. Mohamed, T.M. Salama, J. Colloid Interface Sci. 249 (2002) 104.
[11] M. Muller, G. Harver, R. Prins, Micropor. Mesopor. Mater. 34 (2000) 135.
[12] K. Segawa, S. Mizuno, M. Sugiura, S. Nakata, Stud. Surf. Sci. Catal. 101 (1996) 267.
[13] H. Sasaki, Y. Oumi, K. Itabashi, B. Lu, T. Teranishi, T. Sano, J. Mater. Chem. 1173 (2003).
[14] B. Lu, Y. Oumi, K. Itabashi, T. Sano, Micropor. Mesopor. Mater. 76 (2004) 1.

[15] M.M.J. Treacy, J.B. Higgins, R. Van Ballmoos, Collection of Simulated XRD Powder Patterns for Zeolites, third revised ed., 1996.
[16] S.P. Zhdanov, in: R.F. Gould (Ed.), Advances in Chemistry Series, 101, ACS, Washington Dc, 1971, p. 101.
[17] R. Aiello, F. Crea, E. Nigro, F. Testa, R. Mostowicz, A. Fonsecoz, J.B. Nagy, Micropor. Mesopor. Mater. 28 (1999) 241.
[18] Cid F.J. Gil Liambias, J.L.G. Fierro, A. Lopez, A. Godo, J. Villosenor, J. Catal. 89 (1984) 478.
[19] P.C. Van Geem, K.F. Scholle, G.P.M. Van der Velden, W.S. Veeman, J. Phys. Chem. 91 (1988) 158.
[20] M.W. Urban, Vibrational Spectroscopy of Molecules and Macromolecules on Surfaces, Wiley, Chichester, 1993, 171.
[21] A. Trovarelli, G. Dolcetti, C. de Leitenburg, J. Kaspar, P. Finetti, A. Santoni, J. Chem. Soc. Faraday Trans. 88 (1992) 1311.
[22] S. Braunauer, L.S. Deming, W.S. Deming, E. Teller, J. Amer. Chem. Soc. 62 (1940) 1723.